REVISTA MATÉRIA V.27 N.01

ISSN 1517-7076 artigos e13130, 2022

A new dynamic apparatus for asphalt mix fatigue and stiffness modulus: development, validation and numerical simulations

Breno Salgado Barra[1], Leto Momm[1], Yader Alfonso Guerrero Pérez[1], Alexandre Mikowski[1], Helena Paula Nierwinski[1], Rodrigo Shigueiro Siroma[1], Mai-Lan Nguyen[2], Gary Hughes[3], Gustavo Garcia Momm[4]

[1]Universidade Federal de Santa Catarina (UFSC), Campus de Joinville, Departamento de Engenharias da Mobilidade (EMB), Rua Dona Francisca, 8300, Bloco U, Zona Industrial Norte, CEP: 89.219-600, Joinville, Santa Catarina, Brasil.
[2]Université Gustave Eiffel (UGE), Campus de Nantes, MAST–LAMES, Route de Bouaye, CS 5004, 44340 Bouguenais Cedex, France.
[3]University of California (UC), Department of Physics, Santa Barbara, CA 93106, California, USA.
[4]Petróleo Brasileiro S.A., Petrobrás, Departamento de Engenharia de Produção, Rua Marquês de Herval, 90, Sede UO-BS, Valongo, CEP: 11010-310, Santos, São Paulo, Brasil.
Email: breno.barra@ufsc.br, leto.momm@gmail.com, yagcivil@gmail.com, alexandre.mikowski@ufsc.br helena.paula@ufsc.br, rodrigo_siroma@yahoo.com, mai-lan.nguyen@univ-eiffel.fr, gb.hughes.phd@gmail.com, gustavomomm@yahoo.com

ABSTRACT

The main aim of this paper is to describe the development and validation of a new test apparatus for measuring complex stiffness modulus and fatigue of asphalt mix, so-called FADECOM. Both evaluations are executed with cyclic loading and continuous modes, in order to demonstrate the effectiveness of test results when applied to asphalt pavement design solutions. Results obtained with the new apparatus are compared to existing methods designed on the same mechanical principles, and which are already calibrated and taken as international standardized references. Methods presented in this paper are based on Discrete Fourier Transform (DFT) analysis of data recorded by the test apparatus; a parametric code which executes the analysis was implemented in C++. Interlaboratory comparisons of test results with FADECOM indicate random deviations of approximately 3 microstrains (x 10^{-6} μdef) for determination of fatigue strain at 10^6 cycles, and less than 10% relative difference for complex stiffness modulus. Agreement with FADECOM demonstrates direct applicability of the new method for obtaining accurate data for dynamic numerical simulations comprising asphalt pavement design.

Keywords: Rheological-mechanical performance evaluation. Complex modulus. Fatigue. Asphalt mix. Pavement design.

1. INTRODUCTION

Asphalt pavement is regularly subjected to intense loading and varied environmental stressors. Predicting pavement degradation and useful life requires an acute understanding of rheological-mechanical properties of asphalt mixes at different temperatures and loading frequencies, due to influence these properties exert directly on the thermo-viscoelastic linear behavior of these materials [1-6].

There is a constant need for formulating asphalt mixes, which are able to support the growing, continuous and intense loading axle levels of the traffic fleet worldwide. Ongoing research is focused on the effect of high consistent 10/20 (0.1mm) asphalt binder in increasing the stiffness dynamic complex modulus and resistance to fatigue, which is the main phenomenon responsible for the rupture of pavement structures in the field [7-14].

Test methodologies based on observing mechanical and rheological behavior under cyclic loading of test samples are known to reliably produce laboratory results that closely correlate to field observations [15-20].

Considering the above-mentioned principles, several researches have been carried out aiming to use or to develop apparatuses capable to simulate mechanical and rheological behavior of diverse materials, including asphalt mixes [21-24].

Autor Responsável: Breno Salgado Barra Data de envio: 12/02/2020 Data de aceite: 10/05/2021

10.1590/S1517-707620220001.1330

However, this manuscript presents the first Brazilian-French interlaboratory dynamic Fatigue Development and Complex Stiffness Modulus test apparatus (FADECOM) has been designed by the Pavement Research and Development Group (GDPPav), from Federal University of Santa Catarina (UFSC) - Campus cited at Joinville-SC Brazil. The collaboration has been endeavoring for more than a decade in continuous improvement research on structural adjustment, physical and mathematical models, as well as on numerical simulations, committed to taking into account the technical principles of the French pavement design methodology.

Among particular and notable characteristics of the FADECOM apparatus are its easy portability, despite the robust and stable stainless-steel framework. The apparatus presents possesses the capability to carry out complex stiffness modulus or fatigue tests with four trapezoidal specimens simultaneously, in continuous mode, with displacement amplitude control and generation of sinusoidal loading and displacement signals (Fig. 1), allowing to simulate mechanical efforts in laboratory close to real occurrences in pavement structures in the field [25-28].

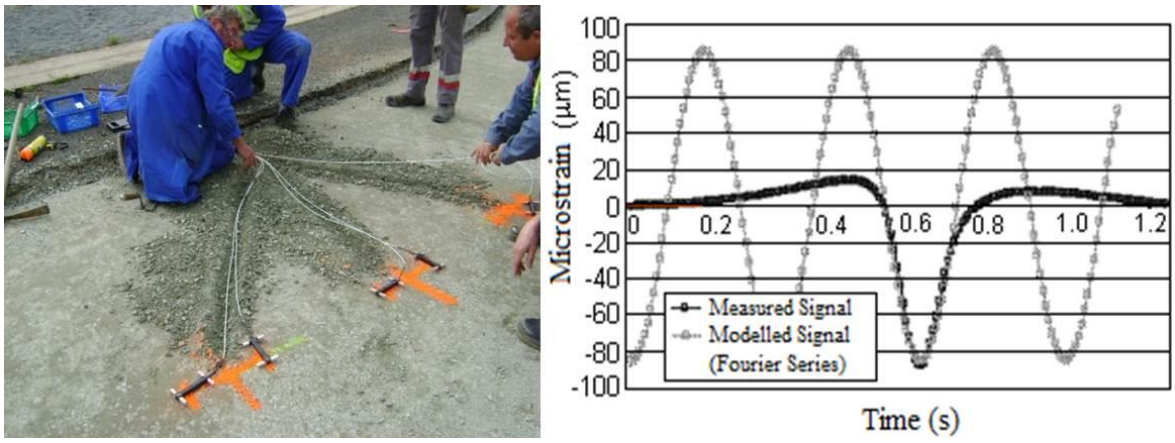

(a) **(b)**

Figure 1: Signal captured with: (a) strain gauges in the field and (b) overlapping a field sinusoidal strain signal calculated using Fourier series [26].

Asphalt mixes that are designed for using as pavement materials must be evaluated for rheological-mechanical performance. A new test apparatus and methods are described for measuring complex stiffness modulus and fatigue of asphalt mixes, based on evaluation of sample frequency response under dynamic loading conditions. Test procedures are formulated from fundamental principles of engineering, in order to ensure that test results represent accurate assessments of relevant phenomena which are observed in practical situations. Results obtained using the new apparatus and methods will therefore produce realistic physical properties which can subsequently be relied upon for modeling and evaluation of asphalt mixtures as pavement materials.

Furthermore, it consists in the first scientific initiative worldwide to propose a design solution capable of carrying out dynamic complex stiffness modulus and fatigue tests in the same apparatus, with a possibility to perform both under distinct environmental conditioning states, i.e., in wet and dry states. It is also a pioneering experience in South America to carry out interlaboratory tests to validate an apparatus, in cooperation with Institut Français des Sciences et Technologies des Transportes, de l'Aménagement et des Réseaux (IFSTTAR), currently Université Gustave Eiffel (UGE).

2. TECHNICAL CHARACTERISTICS OF THE APPARATUS

FADECOM apparatus (Fig. 2) has a solid stainless steel base, which supports a climatic chamber made of polyurethane. The temperature inside this chamber is adjusted by an automatic digital controller that commands two distinct climatic systems: one for heating and another for freezing. Hence, when one of these systems is being adjusted for operation, the other is deactivated automatically, thus, guaranteeing the desired temperature for the tests.

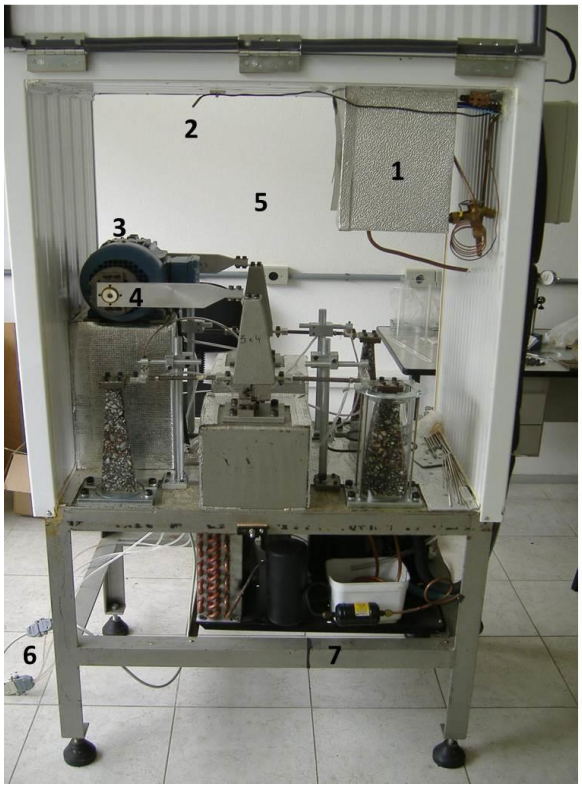

1 – Evaporator unit
2 – Thermocouple
3 – 6-pole induction motor
4 – Eccentric axle
5 – Climatic chamber
6 – Output to data acquisition system
7 – Heating and condensing unit

Figure 2: Overview of the FADECOM apparatus framework.

With this automatic digital controller commanding the heating and condensing unit, it is possible to carry out tests with temperatures ranging from -30ºC to higher than 100ºC. The temperature value during the tests is supplied by 9 thermocouples placed at different points into the chamber with an accuracy of 0.1ºC.

The rotational movement of the eccentric axles generates a force that is transmitted gradually to a set of interlocking pieces until reaching the oscillator rods connected to the specimens.

The force transmitted gradually to the oscillator rods imposes a back and forth displacement on the top part of the specimens, which generates a sinusoidal loading signal from alternating flexion forcing (Fig. 3). The laboratory setup is capable of reproducing strain signal amplitudes measured in the field, i.e., close to real situations, as demonstrated in Fig. 1.

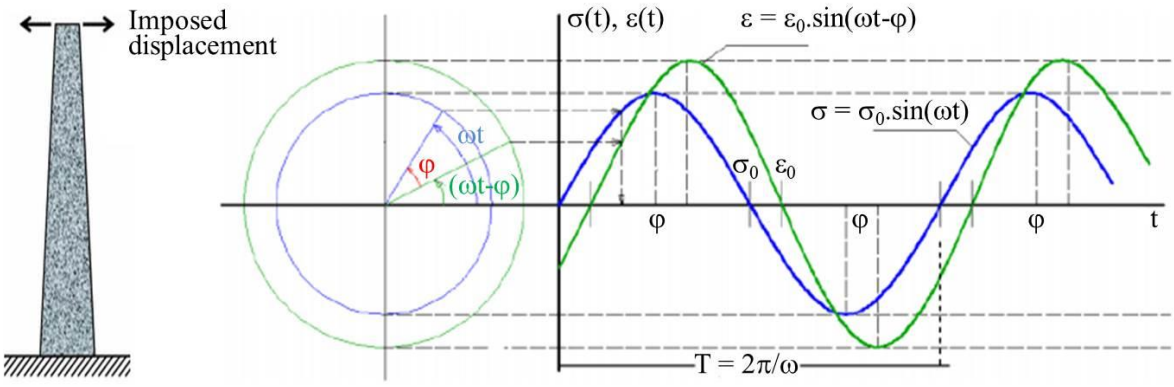

Figure 3: Imposed displacement on the specimens generating sinusoidal loading signal.

Force and displacement signals are captured simultaneously by load cells and Hall Effect sensors, respectively, whereas a frequency inverter is responsible for adjusting the frequency of the tests, which commands a 6-pole induction motor connected to two eccentric axles (Fig. 4).

Figure 4: Detailed view of the: (a) loading cell, (b) Hall Effect sensor, (c) digital automatic controller (left) and frequency inverter (right).

With regards to trapezoidal geometry of the specimen illustrated in Fig. 4, [29] explains that despite the possibility to carry out complex stiffness modulus and fatigue tests with use of prismatic geometries, such as four point bending beams, for instance, a technical inconvenience arises: the section submitted to the highest stresses and, consequently, where collapse normally will occur, is the cantilevered portion, principally during alternated flexion fatigue tests.

Furthermore, during the tests, it is not known the exact distribution and intensity of stresses in the bonding or cantilevered sections. The Saint-Venant Principle can also be cited, which indicates the influence of the cantilevered section is not affected, if the most stressed zone is far from it, allowing to calculate applied stresses taking into account the effective resistance of the materials. Therefore, the most critical section must be designed to occur in the central part of the specimen [30].

Based on the arguments presented, [29] modified the beam prismatic geometry of the specimens initially considered in the research campaign to a profile considered of equal resistance, with parabolic form and being loaded on its free end, i.e. on the top part, generating the most stressed zone in its central part ‘C’ (Fig. 5).

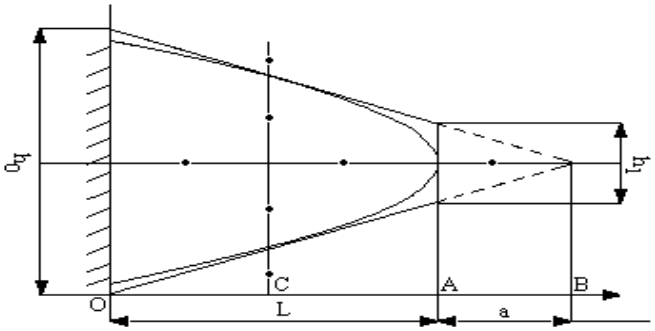

Figure 5: Trapezoidal profile of the specimens [29].

It is also possible to perform complex stiffness modulus and fatigue tests under conditioning states, simulating alternated or continuous wet and dry environmental conditions, submitting the trapezoidal specimens to a prior saturation process into water using a vacuum pomp pressure of 47 kPa ± 5.0% immediately before the beginning of the tests, in order to achieve a saturation degree of the air void content of each specimen.

These conditioning possibilities allow simulating seepage effects that act continuously on the asphalt mixes layers in the field during their life spans, gradually degrading the mechanical performance of these materials, such as: surface tension, aging and stripping [31].

After this pre-conditioning stage, the specimens are kept immersed in water reservoirs during the mentioned tests, affixed on a stainless-steel base specifically designed for this procedure, in order to keep a constant seal and prevent water leakage during the tests (Fig. 6).

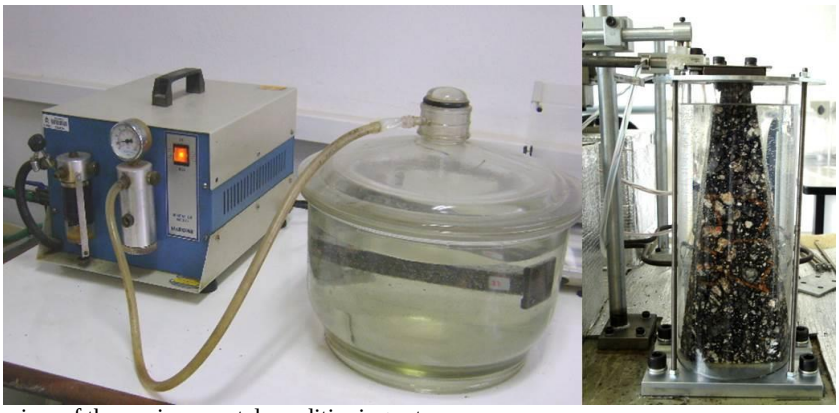

Figure 6: Overview of the environmental conditioning set.

A data acquisition system captures the electrical pulses sent by the load cells and by the Hall Effect sensors with a sample frequency of 640 Hz. A computerized terminal conceived in programming language C^{++} follows a source code flowchart (Fig. 7) to convert these pulses into values of force and displacement for exporting to a graphical interface in Excel sheet in real time, as for complex stiffness modulus (Fig. 8) as for fatigue tests (Fig. 9), using Discrete Fourier Transform (DFT).

According to [32], applying DFT in a set of real and imaginary or complex numbers 'x(n)', considering a constant data set 'i' acquisition interval for a given angular frequency 'ω' rate 'k', it can be assumed as finite the length 'L' of the sequence 'N' uniformly spaced 'k/N' along a period 'T = 2π/ω' (Fig. 4), i.e., restricted to a fixed number of points acquired 'j' (Eqs. 1 to 6).

$$X(\omega) = \sum_{n=0}^{L-1} x(n) e^{-i\omega n} \tag{1}$$

where:

$$\omega_k = \frac{2\pi}{N}k, \text{ for } k = 0,1,\cdots N-1 \tag{2}$$

resulting in:

$$X(k) = X(\omega_k) = \sum_{n=0}^{L-1} x(n)e^{-i2\pi\frac{k}{N}n} \tag{3}$$

which can be written as:

$$X(k) = \sum_{n=0}^{N-1} x(n)e^{-i2\pi\frac{k}{N}n} \tag{4}$$

Thus, discrete samples can be calculated taking into account the base functions of a DFT, i.e., real 'cosinusoidal' and imaginary 'sinusoidal' periodic amplitudes, such as:

$$X(k) = \sum_{n=0}^{N-1} x(i,k)\cos\left(2\pi\frac{k_i}{N}j\right) \tag{5}$$

$$Y(k) = \sum_{n=0}^{N-1} x(i,k)\sin\left(2\pi\frac{k_i}{N}j\right) \tag{6}$$

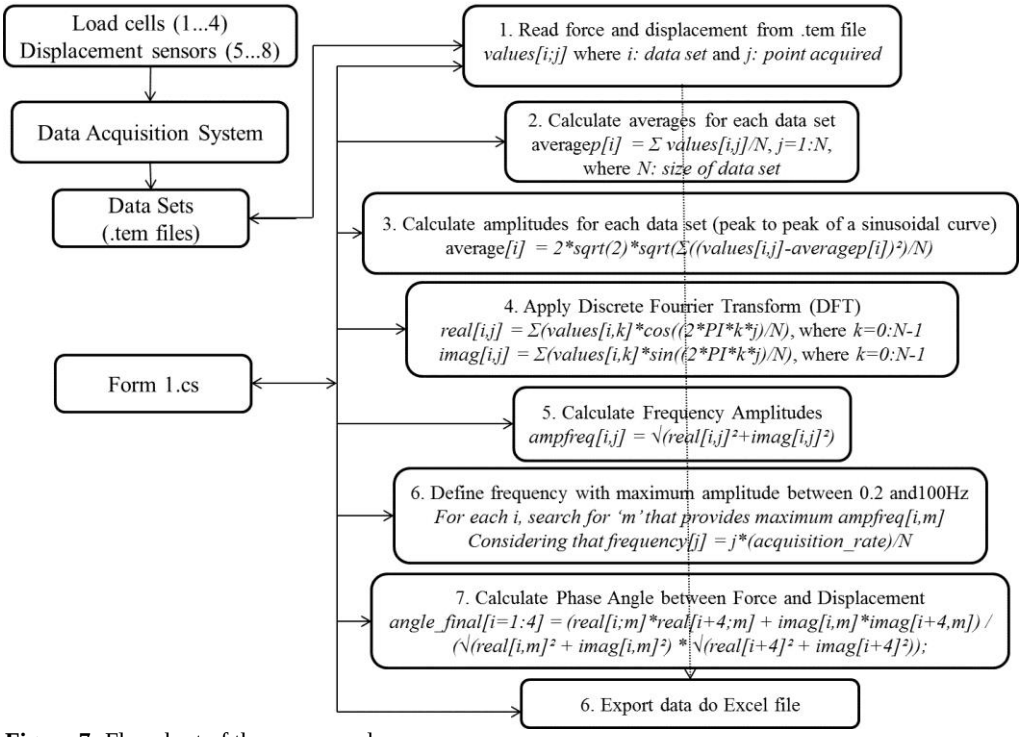

Figure 7: Flowchart of the source code.

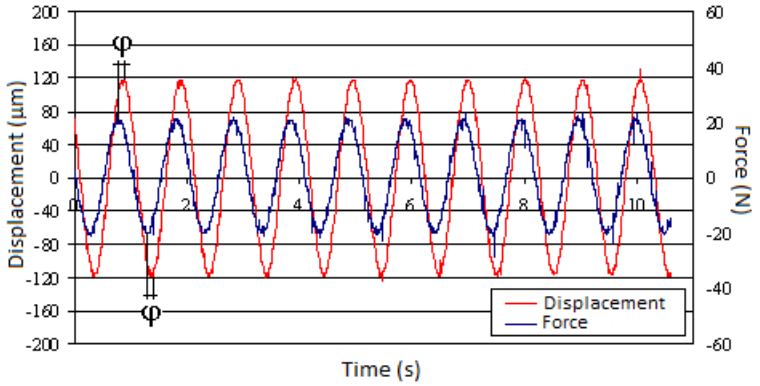

Figure 8: Displacement and force amplitudes captured by the load cells and Hall Effect sensors, evidencing the phase angle (φ) during complex stiffness modulus tests.

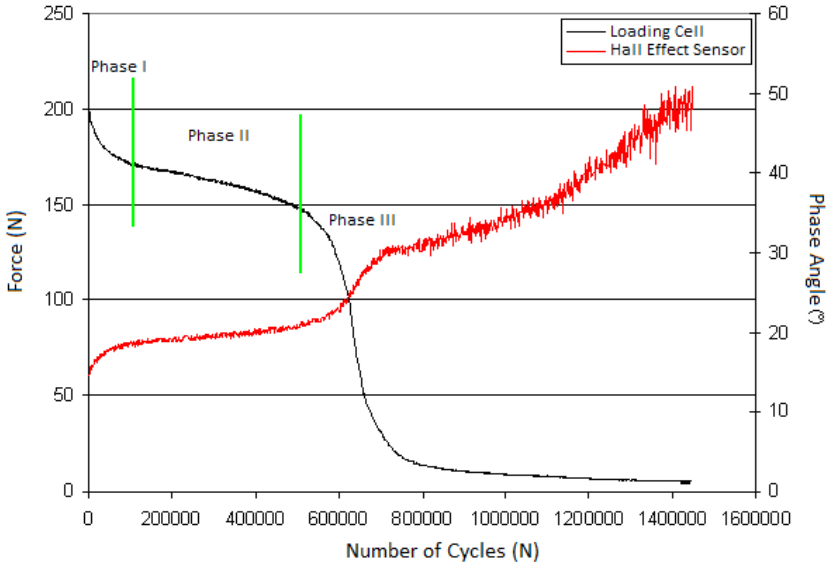

Figure 9: Evolution of the force and phase angle (φ) captured by the load cells and Hall Effect sensors during fatigue tests.

It is important to emphasize the sharpness of the signals captured by the load cells and Hall Effect sensors suitable accuracy of the measurements carried out. In this context, the most important aspects that must be taken into account to obtain sharp signals and qualified data are: a data acquisition system capable to process large number of iterations in a short period of time; force and displacement captors designed with sensors of high sensibility, highlighting the quartz and magnetic technologies; an apparatus framework designed with enough robustness capable to avoid environmental vibrations on the captors, which can cause important noise during the caption of electrical pulses, causing lack of sharpness.

However, there is a perceivable increase of the noise level in phase III of the fatigue tests (Fig. 9), taking into account Hall Effect sensor responses, because at this stage the specimens have reached the structural collapse, in which the displacement amplitude control becomes disordered within the magnetic spectrum of the referred sensors (REF's).

3. VALIDATION PROCESS

In order to attest the accuracy of the tests carried out by FADECOM apparatus, a pioneer scientific cooperation agreement in South America was celebrated in 2015 and renewed in 2017 between GDPPav, representing UFSC, and IFSTTAR, currently Université Gustave Eiffel (UGE), from Nantes, France, to compare the results obtained by both research centers taking into account an interlaboratory campaign considering dynamic complex stiffness modulus and fatigue tests (Fig. 10).

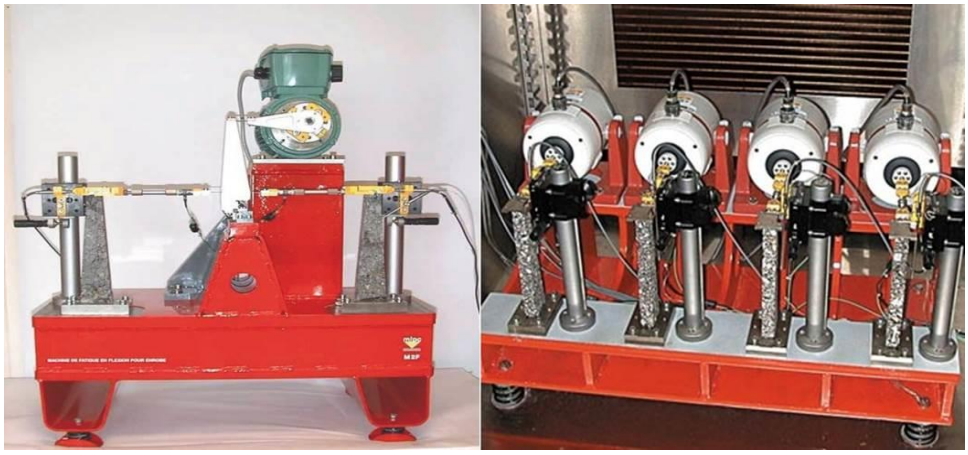

(a) **(b)**

Figure 10: IFSTTAR (a) fatigue and (b) complex stiffness modulus apparatuses.

High modulus asphalt mix, named in France as *Enrobé Bitumineux à Module Élevé* from class 2 (EME2), which comprises many rigorous criteria to be achieved [17], with 0/12.7 mm granitic crushed rock gradation and use of asphalt binder penetration 10/20 (0.1 mm) was chosen to be tested. All trapezoidal specimens were produced in GDPPav laboratory premises, in order to avoid distinct production procedures and to keep the homogeneity of the samples.

The planning of the tests followed the standardized French specifications [17-19], which determine that at least 18 specimens (distributed equally among 3 different strain levels of evaluation) must be tested in a laboratory campaign on the fatigue behavior of a given asphalt mix and at least 4 specimens for carrying out complex stiffness modulus tests [20]. Tests were carried out just in dry state.

In this particular research, 2 sets of 24 specimens were selected, distributed into 3 subsets of 8 units to be tested at each strain level for the fatigue tests, as well as 2 sets of 4 specimens for the complex stiffness modulus tests provided by the same asphalt mix slab (Fig. 11).

(a) **(b)**

Figure 11: Overview of the (a) asphalt mix slab sawing procedure and (b) specimens selected for the tests.

However, to validate each set of specimens to be tested, they must comply with the limits defined by the rigorous statistical criteria of the standardized specifications. These criteria are the variation coefficient based on the results of the constant so-called 'K_ε', related to the geometric dimensions of each specimen (Eq. 7), which must be $\leq$ 1.0%, as well as the standard deviation concerning to the air void content of each set of specimen must be $\leq$ 0.5%. To calculate the air void content, a relation is established between the maximum specific gravity determined by vaccum tests (Fig. 6) and the apparent specific gravity, which considers the mass and volume taken directly from each specimen. If any specimen does not obey one of these criteria, it must be rejected before the beginning of the test and replaced by another suitable unit.

$$K_\varepsilon = \frac{(B-b)^2}{8bh^2\left[\frac{(B-b)(3B-b)}{2B^2} + ln\left(\frac{B}{b}\right)\right]} \quad (7)$$

where 'K_ε' is a constant related to the geometric dimensions of the specimens (mm^{-1}); 'h' is the height of the specimen (mm); 'b' is the small base of the specimen (mm); and 'B' is the large base of the specimen (mm).

The displacement amplitude imposed by the oscillator rods on the top part of the trapezoidal specimens (Fig. 5) is calculated through Eq. (8), which is related to each strain level chosen arbitrarily by the designer.

$$f = \frac{\varepsilon_{max}}{K_\varepsilon} \quad (8)$$

Being the displacement amplitude calculated by $A = 2f$, where 'f' is the half displacement amplitude applied to the small base of the specimen ($x10^{-6}$); 'K_ε' is the constant related to the geometric values of the specimens (mm^{-1}); ε_{max} is the maximum strain level corresponding to a given displacement amplitude ($x10^{-6}$); 'A' is the peak to peak displacement amplitude applied to the small base of the specimen ($x10^{-6}$). It must be remarked that 10^{-6} is the scientific notation for microstrains (μdef).

For fatigue tests, the adjustment of the displacement amplitudes calculated through Eq. (8) (Table 1) was measured with an accuracy of 1.0 μm, using an analogical extensometer, which was placed on the top part of the specimens (Fig. 12).

Figure 12: Adjustment of the displacement amplitudes using an analogical extensometer.

Table 1: Strain levels chosen for fatigue tests and air void content of the asphalt mixes.

Asphalt mix	Temperature of test	Strain level ($x10^{-6}$)			Air void content (%)	Relative standard deviation (%)	Variation Coefficient (%)
		Sets of specimens			Air void content		Kε
		8	8	8			
10/20	10ºC	120	135	150	4.2	0.42	0.31
10/20	30ºC	95	115	135	4.3	0.44	0.34

For all complex modulus tests, the displacement amplitude was calculated and adjusted using the same procedure considered for fatigue tests, but fixed at 40 x 10^{-6} μdef, respecting the standardized maximum limit of 50 x 10^{-6} μdef [20]. Additionally, frequencies of 1 Hz, 3 Hz, 10 Hz and 30 Hz were applied. For each frequency, temperatures of -10ºC, 0ºC, 10ºC, 15ºC, 20ºC, 30ºC, 40ºC and 50ºC were simulated. The displacement amplitudes were gradually regulated by two Allen head screws connected to each eccentric axle (Fig. 2).

With regards to laboratory campaign, Table 2 summarizes the results obtained by the FADECOM and IFSTTAR apparatuses, where 'E_1' is the elastic and 'E_2' the viscous components of the complex stiffness modulus |E*|, while 'φ' is the phase angle measured between force and displacement amplitude signals. The respective standard deviations are also presented (Fig. 8).

Table 2: Comparative results between FADECOM and IFSTTAR apparatuses.

Dynamic Complex Stiffness Modulus Tests								
Test Condition	E_1^1 (MPa)	E_1^2 (MPa)	E_2^1 (MPa)	E_2^2 (MPa)	$\|E^*\|^1$ (MPa)	$\|E^*\|^2$ (MPa)	φ^1 (°)	φ^2 (°)
10°C and 25Hz	24786	24516	2031	2339	24871	24627	4.7	5.5
15°C and 10Hz	20719	19697	2917	3054	20926	19932	8.0	8.8
30°C and 25Hz	12020	10703	4018	3651	12677	11309	18.5	18.6
Relative Standard Deviation (%)								
10°C and 25Hz	1.01	0.99	0.87	1.15	1.01	0.99	0.85	1.17
15°C and 10Hz	1.05	0.95	0.96	1.05	1.05	0.95	0.91	1.10
30°C and 25Hz	1.12	0.89	1.10	0.91	1.12	0.89	0.99	1.01
Fatigue Tests								
Test Condition	ε_6 (x10^{-6})^1				ε_6 (x10^{-6})^2			
10°C and 25Hz	128.8				130.2			
Residual Standard Deviation								
10°C and 25Hz	0.039				0.043			

[1]tests performed with FADECOM apparatus; [2]tests performed with IFSTTAR apparatus.

In this context, it is important to explain the distinction between relative and residual standard deviations, considering the statistical definitions. Relative standard deviation is a standardized measure of dispersion of a probability or frequency distribution. It is often expressed as a percentage and is defined as the ratio of the standard deviation to the mean or its absolute value. It is widely used to express the precision and repeatability of an experimental procedure. On the other hand, residual standard deviation is a dimensionless indicator with regards to difference between a set of experimentally determined and predicted values. Therefore, it expresses how much the data points spread around the regression line, often used in data curation for fatigue tests, aiming to determine the accuracy of the data measured in relation to the predictive model used.

4. CALCULUS OF THE ADMISSIBLE STRAIN

The results obtained in laboratory, more specifically those of complex stiffness modulus and fatigue tests, are directly inserted in numerical simulations by using Huet-Sayegh rheological model [29, 33] (Fig. 13; Eq. 9), as well as in the admissible strain calculus (Eq. 10), with support of the computerized tools Viscoanalyse Ver. Beta [34] and Viscoroute 2.0 [35], considering cyclic loading applications.

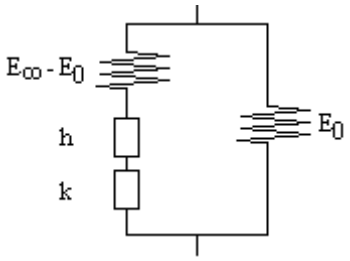

Figure 13: Huet-Sayegh rheological model [29, 33].

$$E^*(\omega) = E_0 + \frac{E_\infty - E_0}{1 + \delta(i\omega t)^{-k} + (i\omega t)^{-h}} \tag{9}$$

where 'i' is the complex number defined by $i^2 = -1$, which indicates the imaginary component of the complex modulus; 'E_∞' is the instantaneous modulus, obtained when $\omega\tau$ tends to the infinite, considering higher frequencies and lower temperatures in loading application conditions; 'E_0' is the static modulus, considering lower frequencies and higher temperatures in loading application conditions; 'τ' concerns the relaxation time of the bumpers 'h' and 'k', thus, a parameter dependent of the time and resembling to a delay time, in which the value varies with the temperature $\tau = \exp(A_0 + A_1.\theta + A_2.\theta^2)$, being θ the temperature and A_0, A_1 and A_2 constants determined experimentally; 'h' and 'k' are the parabolic elements of the model, where for asphalt mixes they comprise the range $0 < k < h < 1$; 'δ' is a dimensionless constant, which depends on the asphalt binder nature and on the aggregate gradation curve; and $\omega = 2\pi f$, being f = loading application frequency (pulsation).

$$\varepsilon\left(NE, \theta_{eq}, f\right) = \varepsilon_6(10°C, 25\ Hz)\left[\frac{E^*(10°C)}{E^*\left(\theta_{eq}\right)}\right]^{\frac{1}{2}}\left(\frac{NE}{10^6}\right)^b k_r k_s k_c \tag{10}$$

where '$\varepsilon(NE, \theta_{eq}, f)$' is the admissible strain of the asphalt mix regarding a given number of loading cycles (NE), equivalent temperature (θ_{eq}) and loading frequency (f); '$\varepsilon_6(\theta, f)$' is the strain level at 10^6 cycles at a given temperature (θ) and loading frequency (f), considered as 10ºC and 25 Hz, respectively, in France; '$(NE/10^6)^b$' is the number of loading cycles predicted to be applicated on the asphalt mix during its service life, in relation to the standard criterion of 10^6 cycles and the slope 'b' concerning the fatigue tests; '$[E^*(\theta)/E^*(\theta_{eq})]^{0,5}$' is the square root between complex stiffness moduli determined at a given temperature (θ) and at a temperature considered as equivalent (θ_{eq}, 15ºC in France); and 'k_r, k_s, k_c' are the failure risk, heterogeneity minority and adjust coefficients, respectively (Eqs. 11 and 12).

$$k_r = 10^{-ub\delta} \tag{11}$$

$$\delta = \left[SN^2 + \left(\frac{c^2}{b^2}\right)Sh^2\right]^{\frac{1}{2}} \tag{12}$$

where 'k_r' is the failure risk coefficient; 'δ' is the standard deviation associated to SN, b, Sh e c; 'SN' is the standard deviation regarding the number of cycles supported by the asphalt mix during fatigue tests log(N); 'u' is the statistical factor (fractile) of the normal series associated to the assumed risk ($\log N/N_{50\%}$); 'b' is the fatigue exponent slope; 'Sh' is the standard deviation concerning the thickness layer all over the pavement structure; and 'c' is the coefficient which correlates the strain (or strength) variation in the pavement structure to random thickness variation Δh ($\log\varepsilon = \log\varepsilon_0$-c.$\Delta h$), in which for ordinary pavement structures is assumed as 0,02 cm^{-1}.

The parameters for defining the fractile 'u' associated to a given percent of failure risk assumed, as well as 'Sh', 'k_s' and 'k_c' are presented in Tables 3, 4, 5 and 6, respectively.

Table 3: Percent of failure risk assumed for asphalt concrete pavement structures regarding the fractile 'u' [36].

Fractile (u)	-0,84	-1,04	-1,28	-1,65	-2,05
Risk (%)	20	15	10	5	2

Table 4: 'Sh' values assumed for asphalt concrete pavement structures regarding the entire bituminous thickness designed [32].

Thickness (cm)	e ≤ 10	10 < e < 15	15 ≤ e
Sh (cm)	1	1 + 0,3(e-10)	2,5

Table 5: Values assumed for the coefficient 'k_s' [36].

Stiffness Modulus (E)	E < 50 MPa	50 MPa ≤ E < 120 MPa	E ≥ 120 MPa
K_s	1/1.2	1/1.1	1

Table 6: Values assumed for the coefficient 'k_c' [36].

Material	k_c
Road base asphalt concrete (GB)	1.3
Bituminous concrete (BB)	1.1
High modulus asphalt concrete (EME)	1.0

It is important to discuss that for calculating the admissible strain at 10^6 loading cycles '$\varepsilon(NE, \theta_{eq}, f)$' with use of Eq. (10), French design methodology considers negligible the direct correspondence between field measurements taken normally at 10 Hz in the bottom of the field asphalt concrete layers and those determined at 25 Hz in laboratory tests, taking into account usual temperatures of service [36].

However, the coefficient 'k_c' is predicted in the above-mentioned Eq. (10), in order to adjust the mathematical model used in laboratory to the mechanical behavior evaluated in the field, since true-scale pavement section tests, which have been carried out over three decades with a fatigue carroussel framework, being responsible to assure a narrow field/laboratory ratio (Table 6), thus, adjusting eventual scatters between measurements realized at 10 Hz and at 25 Hz [37].

These technical procedures made it possible to determine the viscoelastic linear parameters and mechanical behavior in pavement structure design regarding the asphalt mix tested.

5. NUMERICAL SIMULATIONS ON DESIGNING PAVEMENT STRUCTURE

For demonstrating the practical applicability of the mechanical and rheological parameters determined with use of the FADECOM apparatus, it was carried out numerical simulations comprising a pavement structure designed based on French methodology concepts [36], considering the following technical conditions: annual average daily traffic flow (MJA) of 6.000 heavy trucks (class TC8) with 130 kN double-wheeling standard single axle load each, applying cyclic loadings at 72 km/h.

A cumulative traffic (NE) of 8.34 x 10^7 was predicted to be supported along 30 years, assuming 15% of failure risk (k_r = 0.887 at 10°C and 25 Hz), besides 1/1.1 related to heterogeneity minority (k_s) and 1.0 to adjust (k_c) coefficients mentioned earlier in section 4.

They were considered a foundation platform from class 3 (PF3) with a stiffness modulus of 100 MPa in soil treated with lime, while sub-base and base layers with high modulus asphalt mix or also so-called *Enrobé Bitumineux à Module Élevé* class 2 (EME2), taking into account the formulation tested in the experimental campaign carried out and described in section 3. For EME2, thickness layers from 9.0 cm to 13.0 cm were simulated following standardized recommendations [38].

Rheological parameters of the asphalt mix EME2 were determined with use of Huet-Sayegh viscoelastic linear model (Eq. 9) simulated in the computerized tool so-called Viscoanalyse Ver. Beta (Table 7), considering results from complex modulus tests presented in Table 2. Complex modulus and fatigue test results used in the numerical simulations are compiled in Table 8.

Table 7: Rheological Parameters from Huet-Sayegh Model for EME2.

Huet-Sayegh Model Parameters	Results for EME2
$E\infty$	32215.90 MPa
E_0	139.938 MPa
K	0.205
H	0.65009
δ	1.25729
A_0	4.45615
A_1	-0.345861
A_2	0.0014058
τ	0.65009

Table 8: Complex Modulus and Fatigue Test Results for EME2.

Test Condition	Complex Modulus	Fatigue		
	|E*| (MPa)	ε_6 (x 10^{-6})	SN	1/b
10°C e 10Hz	23612	-	-	-
15°C e 10Hz	20926	-	-	-
10°C e 25Hz	-	128.8	0.039	0.14

Furthermore, according to [36], when it is being designed an asphalt concrete pavement structure able to support heavy traffic flows, it must be evaluated not only the admissible tensile strain in the bottom of the deepest asphalt layer '$\varepsilon(NE,\theta_{eq}, f)$' calculated by Eq. (10), but also the admissible vertical compression strain '$\varepsilon_{z,ad}$' on the top of the foundation platform (PF), as defined in Eq. (13).

$$\varepsilon_{z,ad} = 0{,}012(NE)^{-0{,}222} \tag{13}$$

where '$\varepsilon_{z,ad}$' is the admissible vertical compression strain on the top of the foundation platform (PF); and 'NE' is the cumulative traffic concerning 130 kN standard double-wheeling single axle load.

The development of numerical simulations interacting Huet-Sayegh rheological viscoelastic linear model and mechanical behavior at cyclic loading applications on the designed pavement structure was carried out with use of computerized tool so-called Viscoroute 2.0, in which the results are presented in Table 9 and illustrated by Fig. 14.

Table 9: Results obtained in numerical simulations.

Test condition (numerical simulation routines)	Thickness (cm)	Admissible calculated values		Numerical simulation results	
		$\varepsilon(NE, \theta_{eq}, f)$ (x 10^{-6})	($\varepsilon_{z,ad}$) (x 10^{-6})	(ε_t) (x 10^{-6})	(ε_z) (x 10^{-6})
ε_6 = 10ºC and 25Hz E*(θ) = 10ºC and 10Hz E*(θ_{eq}) = 15ºC and 10Hz	9.0cm/9.0cm*	59.32	-209.26	55.08	-56.49

Legend:

*Thickness (cm) in order: base/sub-base asphalt layers (2 layers).

ε_t : tensile strain in the bottom of the deepest asphalt layer.

$\varepsilon(NE,\theta_{eq},f)$: admissible tensile strain in the bottom of the deepest asphalt layer calculated with use of Equation 3.

ε_z : compression strain on the top of the platform foundation.

$\varepsilon_{z,ad}$: admissible compression strain on the top of the platform foundation, calculated with use of Equation 4.

Signal convention of Viscoroute 2.0: (+) tensile and (-) compression.

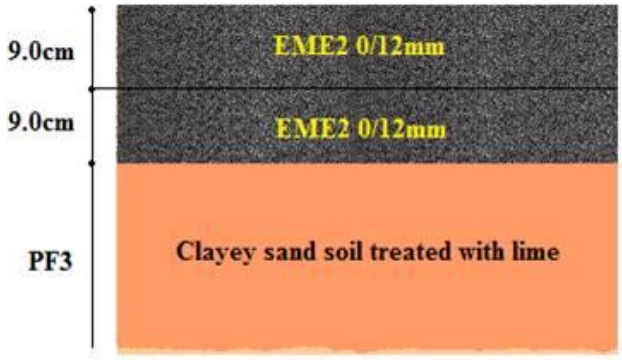

Figure 14: Pavement structure designed after numerical simulation routine.

The results presented in Table 9 indicate numerical simulation routine values of 'ε_t' and 'ε_z' minor than the admissible calculated limits '$\varepsilon(NE,\theta_{eq},f)$' and '$\varepsilon_{z,ad}$', considering initial asphalt layer thicknesses of 9.0 cm, as well as complex modulus ratio '$[E^*(\theta)/E^*(\theta_{eq})]^{0,5}$' with $E^*(\theta)$ = 10ºC and $E^*(\theta_{eq})$ = 15ºC, both determined at 10 Hz, and fatigue 'ε_6' obtained at 10ºC and 25 Hz, thus, being in accordance to French pavement design standardized principles predicted in [32], attending the technical scope proposed to this research.

6. CONCLUSIONS

Analyzing data presented in this research, it is possible to infer that the variability of results is less than 5.0% for dynamic (complex) stiffness modulus (|E*|), less than 1.2% for phase angle (º) and 1.0% maximum for fatigue strain at 10^6 loading cycles (ε_6), when compared with the values determined by the FADECOM and IFSTTAR apparatuses. These trends are strongly lower than the standard deviation tolerances established by the French methodology, i.e., around 10% maximum for stiffness modulus and 3.0 ($x10^{-6}$) for ε_6 ($x10^{-6}$), demonstrating greatly improved accuracy of the FADECOM apparatus and its actual feasibility to be applied in pavement design solutions.

7. ACKNOWLEGMENTS

We would like to thank to Université Gustave Eiffel (UGE) from Nantes, France, by the continuous scientific cooperation agreement with our Group of Research and Development in Pavement (GDPPav). Also to Petrobrás S.A., for financing the construction of the FADECOM apparatus via Cooperation Agreement Term 0050.0075479.12.9 and Project nº4600373381, as well as to Gustavo Momm by the decisive and effective collaboration during the mechanical and logical development of the FADECOM apparatus.

8. REFERENCES

[1] PINTARELLI, M.G., MELO, J.V.S., "Influence of Haversine and Sinusoidal Wave Load on Estimating Fatigue Life of Asphalt Layers." doi.org/10.1061/(ASCE)MT.1943-5533.0002700. Journal of Materials in Civil Engineering, v. 31, n. 8. 2019.

[2] ALMEIDA, A.J., MOMM L., TRICHÊS, G., *et al.* "Evaluation of the influence of water and temperature on the rheological behavior and resistance to fatigue of asphalt mixtures." doi.org/10.1016/j.conbuildmat.2017.10.030. Construction and Building Materials, 158, pp. 401-409. 2018.

[3] QUINTERO, C.F.Q., MOMM, L., LEITE, L.F.M., *et al.*, "Effect of asphalt binder hardness and temperature on fatigue life and complex modulus of hot mixes." doi.org/10.1016/j.conbuildmat.2016.03.161. Construction and Building Materials, 114, pp.755–762. 2016.

[4] ISLAM, R., TAREFDER, R.A., "Developing Temperature-Induced Fatigue Model of Asphalt Concrete for Better Prediction of Alligator Cracking." doi.org/10.1061/(ASCE)MT.1943-5533.0001477. Journal of Materials in Civil Engineering, v. 28, n. 5. 2016.

[5] NGUYEN, M-L., DI BENEDETTO, H., SAUZÉAT, C., "Crack propagation characterization of bituminous mixtures using a four-point bending notched specimen test." doi.org/10.1080/14680629.2015.1063535. Road Materials and Pavement Design (RMPD), v. 17, n. 1, pp. 70-86. 2015.
[6] LUNDSTRÖM, R., ISACSSON, U., AND EKBLAD, J., "Investigations of stiffness and fatigue properties of asphalt mixtures." Journal of Materials Science, 38, pp. 4941-4949. 2003.
[7] BABADOPULOS, L.F.A.L., OROZCO G., SAUZÉAT, C., *et al.* "Reversible phenomena and fatigue damage during cyclic loading and rest periods on bitumen." doi.org/10.1016/j.ijfatigue.2019.03.008. International Journal of Fatigue, 124, pp. 303-314. 2019.
[8] ZHU, J., ZHANG, W., "Probabilistic fatigue damage assessment of coastal slender bridges under coupled dynamic loads." doi.org/10.1016/j.engstruct.2018.03.073. Engineering Structures, 166, pp. 274-285. 2018.
[9] WU, H., HUANG, B., SHU, X., "Characterizing Fatigue Behavior of Asphalt Mixtures Utilizing Loaded Wheel Testers." doi.org/10.1061/(ASCE)MT.1943-5533.0000791. Journal of Materials in Civil Engineering, v. 26, n. 1, pp. 152-159. 2014.
[10] GRAEFF, A.G., PILAKOUTAS, K., NEOCLEOUS, K., *et al.* "Fatigue resistance and cracking mechanism of concrete pavements reinforced with recycled steel fibres recovered from post-consumer tyres." doi.org/10.1016/j.engstruct.2012.06.030. Enginerring Structures, 45, pp. 385-395. 2012.
[11] DOMEC, V., "Endommagement par fatigue des enrobés bitumineux em condition de trafic simulé et de température." Thèse de Docteur. Université de Bordeaux I, p. 426, 2005.
[12] DI BENEDETTO, H., PARTL, M.N., FRANCKEN, L., *et al.* "Stiffness testing for bituminous mixtures", Materials and Structures/Matériaux et Constructions, 34, pp. 66-70. 2001.
[13] MOMM, L., Estudo dos Efeitos da Granulometria Sobre a Macrotextura Superficial do Concreto Asfáltico e Seu Comportamento Mecânico. PhD Thesis presented to Polytecnhical School of University of São Paulo (USP), p. 357, 1998.
[14] RUDENSKY, A.V., "Asphalt concrete fatigue properties." *Proc., 5th Int. RILEM Symposium*. Mechanical Tests for Bituminous Materials (MBTM): Recent Improvements and Future Prospects. Lyon, France, pp. 1058-1066. 1997.
[15] OTTO, G.G., SIMONIN, J-M., PIAU, J-M., *et al.* "Weigh-in-motion (WIM) sensor response model using pavement stress and deflection." doi.org/10.1016/j.conbuildmat.2017.08.085. Construction and Building Materials, 156, pp. 83-90. 2017.
[16] CHKIR, R., BODIN, D., PIJAUDIER-CABOT, G., *et al.* "An inverse analysis approach to determine fatigue performance of bituminous mixes." doi.org/10.1007/s11043-009-9096-7. Mechanics of Time-Dependent Materials, 13, pp. 357-373. 2009.
[17] MANUEL, L.P.C., "*Manuel LPC d'aide à la formulation des enrobés."* Groupe de Travail RST Formulation des enrobés, 320p. Laboratoire Central des Ponts et Chaussées. Paris, France. 2007.
[18] SIMONIN, J-M., VILLAIN, G., HORNYCH, P., "Monitoring of artificial defects within a pavement structure with ultrasonic pulse echo." *Proc., Non-Destructive Technique (NDT) Conference*. Berlin, Germany; https://www.researchgate.net/publication/280934917. 2015.
[19] AFNOR NF EN 12697-24, "Mélanges Bitumineux: Méthode d'Éssai pour Mélange Hydrocarboné à Chaud - Partie 24: Essai par Flexion à Flèche Constante." 32p. Association Française de Normalisation. Paris, France. 2012.
[20] AFNOR NF EN 12697-26, "Mélanges Bitumineux: Méthode d'Éssai pour Mélange Hydrocarboné à Chaud - Partie 26: Module de Rigidité." 40p. Association Française de Normalisation. France. 2012.
[21] LAGES, M.S., ABRÃO , A.M., SANTOS, A.J., *et al.* "Desenvolvimento de uma máquina para ensaio de fadiga por flexão"., artigo e-12301, https://doi.org/10.1590/s1517-707620190001.0638. Revista Matéria, v. 24, n. 1, 12 p., 2019.
[22] BOEIRA, F.D., PINHEIRO, G. S., SPECHT, L.P., *et al.* "Projeto e implementação de ensaio de fadiga por tração-compressão direta (uniaxial) para avaliação de dano em misturas asfálticas"., artigo e-12148, https://doi.org/10.1590/S1517-707620180003.0482. Revista Matéria, v. 23, n.3, 14 p., 2018.
[23] CENTOFANTE, R., SPECHT, L.P., ALMEIDA JUNIOR, P.O.B., *et al.* "Avaliação do comportamento de misturas asfálticas recicladas a quente com inserção de material fresado"., artigo e-12178, , https://doi.org/10.1590/S1517-707620180003.0512 , Revista Matéria, v. 23, n.3, 19 p. 2018.
[24] CARVALHO, I.S., REZENDE, L.R., SILVA, J.P.S., *et al.* "Estudo do Concreto Asfáltico Estocável"., artigo e-12881, https://doi.org/10.1590/s1517-707620200004.1181 . Revista Matéria, v. 25, n. 4, 22 p. 2020.
[25] BARRA, B., MOMM, L., GUERRERO, Y., *et al.*"Fatigue behavior of dense asphalt mixes in dry and environmental-conditioning states", Construction and Building Materials, 29, pp. 128-134. 2012.
[26] PERRET, J., "Déformation des couches bitumineuses au passage d'une charge de trafic." Thèse de Doctorat. École Polytechnique Fédérale de Lausanne (EPFL). Lausanne, Suisse. 2003.

[27] HECK, J-V., Modélisation des déformations réversibles et permanentes des enrobés bitumineux - Application à l'ornièrage des chaussées. Thèse de Doctorat. Université de Nantes. 2001.
[28] DE LA ROCHE, C., ODEON, H., "Expérimentation USAP/LCPC/Shell - Fatigue des Enrobés - Phase 1 - Rapport de Synthèse." Document de Recherche LCPC, sujet nº2.01.10.4. 1993.
[29] HUET, C., "Étude par une méthode d'impédance du comportement viscoélastique des materiaux hydrocarbonés." Thèse de Docteur. Faculté des Sciences de l'Université de Paris, France. 1963.
[30] DI BENEDETTO, H., DE LA ROCHE, C., "State of the Art on Stiffness Modulus and Fatigue of Bituminous Mixtures", in Bituminous Binders and Mixtures: state of the art and RILEM interlaboratory tests on mechanical behavior and mix design. E&FN Spon, Ed. L. Francken, 17p. 1998.
[31] BARRA, B., "Avaliação da Ação da Água no Módulo Complexo e na Fadiga de Misturas Asfálticas Densas." PhD Thesis presented to Federal University of Santa Catarina (UFSC), 327p. Florianópolis, Brazil. 2009.[22] Barra, B., Momm, L., Guerrero, Y. and Bernucci, L., "Fatigue behavior of dense asphalt mixes in dry and environmental-conditioning states", Construction and Building Materials, 29, pp. 128-134. 2012.
[32] HUGHES, G.B., *Frequency-Domain Analysis with DFTs.* 1st Ed. Vol. PM282. ISBN: 9781510616097. Spie Press Book. 230 pages. USA. 2017.
[33] SAYEGH, G., "Contribution à l'étude des propriètés viscoélastiques des bitumes purs et des bétons bitumineux." Thèse de Docteur Ingénieur. Faculté des Sciences de Paris. 206p. France. 1965.
[34] CHAILLEUX, E., *Note d'utilisation de l'application logicielle viscoanalyse*. Institut Français des Sciences et Technologies des Transportes, de l'Aménagement et des Réseaux (IFSTTAR). France. 2007.
[35] CHABOT, A., CHUPIN, O., DELOFFRE, L., *et al.* "Viscoroute 2.0: A tool for the simulation of moving load effects on asphalt pavement." doi.org/10.1080/14680629.2010.9690274. 2010. Road Materials and Pavement Design (RMPD), v. 11, n. 2, pp. 227-250.
[36] GUIDE TECHNIQUE, *French Design Manual for Pavement Structures (English Version)*. Service d'Études Techniques des Routes et Autoroutes (SETRA) and Laboratoire Central des Ponts et Chaussées (LCPC), 248 p. Paris, France. 1998.
[37] EL ABD, A., "Développement d'une méthode de prédiction des déformations de surface des chaussées à assises non traitées." Thèse de Docteur. Université de Bordeaux I. 2006.
[38] CATALOGUE LCPC/SETRA, *Catalogue des Structures Types de Chaussées Neuves: Réseau Routière National*. Laboratoire Central des Ponts et Chaussées (LCPC) en partenariat avec le Service d'Étude Technique des Routes et Autoroutes(SETRA), Paris, France. 1998.

ORCID

Breno Barra	https://orcid.org/0000-0003-2212-8163
Leto Momm	https://orcid.org/0000-0003-0243-7903
Yader Guerrero Pérez	https://orcid.org/0000-0002-4048-050X
Alexandre Mikowski	https://orcid.org/0000-0002-5348-8420
Helena Nierwinski	https://orcid.org/0000-0002-6286-2250
Rodrigo Siroma	https://orcid.org/0000-0003-3919-0879
Mai-Lan Nguyen	https://orcid.org/0000-0001-8966-5209
Gary Hughes	https://orcid.org/0000-0003-4739-8493
Gustavo Momm	https://orcid.org/0000-0002-3463-0719